

Time-resolved analysis of particle emissions from residential biomass combustion – Emissions of refractory black carbon, PAHs and organic tracers



Ingeborg E. Nielsen ^{a, b, *}, Axel C. Eriksson ^{c, d}, Robert Lindgren ^e, Johan Martinsson ^{d, f}, Robin Nyström ^e, Erik Z. Nordin ^c, Ioannis Sadiktsis ^g, Christoffer Boman ^e, Jacob K. Nøjgaard ^{a, b}, Joakim Pagels ^c

^a Department of Environmental Science, Aarhus University, Box 358, DK-4000 Roskilde, Denmark

^b Arctic Research Centre, Aarhus University, DK-8000 Aarhus, Denmark

^c Division of Ergonomics and Aerosol Technology, Lund University, Box 118, SE-221 00 Lund, Sweden

^d Division of Nuclear Physics, Lund University, Box 118, SE-221 00 Lund, Sweden

^e Thermochemical Energy Conversion Laboratory, Umeå University, SE-901 87 Umeå, Sweden

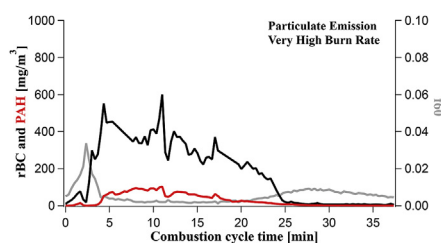
^f Centre for Environmental and Climate Research, Ecology Building, Lund University, SE-223 62 Lund, Sweden

^g Department of Environmental Science and Analytical Chemistry, Stockholm University, SE-106 91 Sweden

HIGHLIGHTS

- Time-resolved analysis of wood stove emissions as a function of burn rate.
- Fuel addition - > Low temperature pyrolysis - > High OA emissions.
- Flaming Combustion - > rBC emissions with organic coating.
- Very high burn rate - > unchanged m/z 60, elevated rBC and OA emissions and very strongly elevated PAH emissions.
- High burn rate - > air-starved combustion zone - > reduced temperature - > slow conversion of PAHs to rBC - > high PAH emissions.

GRAPHICAL ABSTRACT



ARTICLE INFO

Article history:

Received 15 December 2016

Received in revised form

18 June 2017

Accepted 19 June 2017

Available online 20 June 2017

Keywords:

Black carbon

PAHs

Residential biomass combustion

SP-AMS

Levoglucosan

ABSTRACT

Time-resolved particle emissions from a conventional wood stove were investigated with aerosol mass spectrometry to provide links between combustion conditions, emission factors, mixing state of refractory black carbon and implications for organic tracer methods. The addition of a new batch of fuel results in low temperature pyrolysis as the fuel heats up, resulting in strong, short-lived, variable emission peaks of organic aerosol-containing markers of anhydrous sugars, such as levoglucosan (fragment at m/z 60). Flaming combustion results in emissions dominated by refractory black carbon co-emitted with minor fractions of organic aerosol and markers of anhydrous sugars. Full cycle emissions are an external mixture of larger organic aerosol-dominated and smaller thinly coated refractory black carbon particles. A very high burn rate results in increased full cycle mass emission factors of 66, 2.7, 2.8 and 1.3 for particulate polycyclic aromatic hydrocarbons, refractory black carbon, total organic aerosol and m/z 60, respectively, compared to nominal burn rate. Polycyclic aromatic hydrocarbons are primarily associated with refractory black carbon-containing particles. We hypothesize that at very high burn

* Corresponding author. Department of Environmental Science, Aarhus University, Frederiksborgvej 399, 4000 Roskilde, Denmark.

E-mail address: ien@envs.au.dk (I.E. Nielsen).

rates, the central parts of the combustion zone become air starved, leading to a locally reduced combustion temperature that reduces the conversion rates from polycyclic aromatic hydrocarbons to refractory black carbon. This facilitates a strong increase of polycyclic aromatic hydrocarbons emissions. At nominal burn rates, full cycle emissions based on m/z 60 correlate well with organic aerosol, refractory black carbon and particulate matter. However, at higher burn rates, m/z 60 does not correlate with increased emissions of polycyclic aromatic hydrocarbons, refractory black carbon and organic aerosol in the flaming phase. The new knowledge can be used to advance source apportionment studies, reduce emissions of genotoxic compounds and model the climate impacts of refractory black carbon, such as absorption enhancement by lensing.

© 2017 The Authors. Published by Elsevier Ltd. This is an open access article under the CC BY license (<http://creativecommons.org/licenses/by/4.0/>).

1. Introduction

Biomass combustion is widely used for energy production, cooking and residential heating. Advantages include potentially low net emissions of greenhouse gases in addition to being an economically favorable energy source. However, biomass combustion is inevitably associated with emissions of volatile and particulate species that affect climate (Bond et al., 2013) and human health (Naeher et al., 2007; Sigsgaard et al., 2015). Furthermore, individual emissions are strongly influenced by user behavior in terms of fuel and stove use (Wöhler et al., 2016). The design of the stove and the type of wood (e.g., wood species, log size, amount of humidity) influence particulate emissions.

Operating a wood stove with wood batches that are too large, or using very dry wood combined with small log sizes may lead to a burn rate that is too high for the particular stove, resulting in strongly increased emissions of polycyclic aromatic hydrocarbons (PAH) (Elsasser et al., 2013; Eriksson et al., 2014; Pettersson et al., 2011), which are known genotoxic compounds (Sarigiannis et al., 2015). Moreover, the batch-fired nature of the wood stove operation leads to substantial variations in emission levels and characteristics over the cycle (Eriksson et al., 2014; Leskinen et al., 2014; Martinsson et al., 2015; Pagels et al., 2013). The operation of wood stoves is inherently associated with a substantial variation between replicates, which reflects the difficulty of controlling the burning process. On a mass basis, the toxicity of wood combustion particles is believed to be at least as potent as other combustion sources (Boman et al., 2003). The transient nature of the combustion cycles calls for highly time-resolved online sampling and analysis techniques to characterize emission levels. Time-resolved aerosol mass spectrometry (AMS) has identified distinct relationships between combustion conditions/phases, different fuels and the chemical composition of emissions (Corbin et al., 2015a; Heringa et al., 2012; Weimer et al., 2008). For example, organic aerosol (OA) mass spectra have been linked to the chemistry of wood pyrolysis (Corbin et al., 2015b). Additionally, the PAH and OA emissions are elevated at different burn phases, which has implications for recommended burn practices and future emission legislation (Eriksson et al., 2014).

Black carbon (BC) is a valuable air quality indicator to evaluate the health risks of ambient air impacted by combustion particles (Janssen et al., 2011). BC also affects the climate by absorbing solar radiation where the degree of coating on the BC alters the absorption. As an example, internally mixed OA with BC have been shown to substantially enhance the light absorption of BC from residential combustion sources (Liu et al., 2015). A recent study found that a transition from brown carbon (BrC) to BC dominated the absorption of the emissions from the fuel addition to the flaming phase (Martinsson et al., 2015). Little previous information exists regarding the time-resolved emissions of BC and their relationship to OA, PAHs and other organic sub-classes, such as

monosaccharides (e.g., levoglucosan) at elevated burn rates. The recently developed soot particle time-of-flight aerosol mass spectrometer (SP-AMS) (Onasch et al., 2012) is capable of size-resolved detection of particulate refractory black carbon (rBC) in addition to non-refractory OA and a few key sub-classes as has been recently shown for wood stove emissions at nominal operation (Corbin et al., 2015b). PAHs are precursors of soot/rBC (Wang, 2011) and it is well known from biomass gasification studies that reduced combustion/gasification temperatures can lead to elevated PAH emissions (Milne et al., 1998). However, such mechanisms have rarely been used to interpret PAH emissions from residential biomass combustion.

Levoglucosan is a pyrolysis product of cellulose (Simoneit, 2002) and a widely used specific tracer for wood combustion emissions (Gelencser et al., 2007; Genberg et al., 2011; Yttri et al., 2011). However, a number of studies have questioned its use as a tracer because levoglucosan is susceptible to atmospheric degradation when it reacts with hydroxyl radicals, in particular during the summer with elevated OH concentrations (Hennigan et al., 2010, 2011). Additionally, the use of the levoglucosan fragment ion m/z 60 ($C_2H_4O_2^+$) in the AMS spectrum may overestimate levoglucosan, since other anhydrous sugars and other compounds formed during wood combustion/pyrolysis as well as secondary organic aerosol (SOA) may contribute to this fragment (Heringa et al., 2011). Still, levoglucosan is a specific tracer for wood combustion and may serve as a marker if its limitations are carefully addressed. The amount of levoglucosan emitted is variable and depends on factors such as combustion conditions and type of fuel (Engling et al., 2006; Fine et al., 2002, 2004; Zdrahal et al., 2002). This causes increased uncertainty in source apportionment methods. Thus, there is a great need to conduct bottom-up source inventories from specific wood stoves and combustion conditions in order to mitigate this uncertainty. Previous studies have investigated the variability of m/z 60 and its fraction of OA (f_{60}) as a function of combustion phase and fuel (Elsasser et al., 2013; Weimer et al., 2008). It is crucial to understand the variability of these parameters and their ratios during different burning conditions and phases in order to evaluate source profiles of residential wood combustion for use in source apportionment.

In this study, we investigate the emissions of the air quality parameters of rBC_e (equivalent refractory black carbon, explained in Section 2.3), PAHs, OA and m/z 60 over an extended range of burn rates using a conventional wood stove. We also report emission factors for the main burn phases of each batch. We investigate the relationship between PAH and rBC_e emissions and discuss the combustion conditions leading to deteriorated emission levels at high burn rates. We investigate relationships between OA and m/z 60 as a function of the burn rate and of the OA emission factor. We additionally illustrate that size-resolved analysis with the SP-AMS can be used to deduce the major particle types occurring in the emissions, including the mixing state of relevance for direct

radiative forcing. We validate the SP-AMS for the quantification of PAHs and rBC by comparison with reference methods.

2. Materials and methods

2.1. Experimental setup and combustion facilities

The experiments were carried out using a conventional natural-draft wood stove with a nominal heat output of 9 kW. The stove model was commonly installed in the Nordic countries during the 1990s. The stove has been used in previous studies as described in detail elsewhere (Eriksson et al., 2014; Pettersson et al., 2011). In all cases, the wood used was typical Scandinavian silver birch (*Betula pendula*). The ash content of the fuel was 0.42%. More information on the characteristics of the wood, including the ash composition, is given in Table S1 in the Supplementary Material (SM). The wood stove was operated in three different burning modes: nominal burn rate (NB), high burn rate (HB), and very high burn rate (VHB). The NB mode followed the manufacturer's recommendations for the stove. It was loaded with 2.5 kg fuel per batch (3 wood logs, 0.6–1.1 kg/log), with a moisture content of 15%. Both HB and VHB included higher fuel loads, while staying within a plausible and realistic range (HB: 3.5 kg/batch, 5–6 wood logs, 0.6–0.7 kg/log, moisture content 7%. VHB: 4 kg/batch, 8–9 wood logs, 0.4–0.5 kg/log, moisture content 7%). The VHB case was used to simulate the behavior of the stove and the emissions when overloading the stove and getting high burn/air-starved rate conditions. The parameters applied in this study were by no means extreme. During NB, O₂ in the flue gas was rather stable around 10% (8–12%) with CO levels <500 ppm. During HB, O₂ in the flue gas varied more in the beginning of the intermediate phase with shorter periods of high burn rates and “air-deficient” conditions, with O₂ around 5% and CO peaks up to 15,000 ppm. Finally at VHB, periods with intensive and air-starved conditions were extended, with O₂ decreasing below 2% and very high CO peaks (>30,000 ppm). As seen in Table S2, the burn rate (kg_{wood}/h) increased from NB (3.1) to HB (4.5) and VHB (5.3). The corresponding flue gas temperature was highest during VHB and lowest during NB. Thus, the variations in these combustion-related parameters are in line with the variations that were intended in the experimental matrix that was applied in this study.

Flue gas from the stove was emitted into a chimney stack where the sampling took place. CO and O₂ concentrations were measured directly from the undiluted flue gas by electrochemical sensors with a flue gas analyzer (Testo AG, Lenzkirch, Germany). The aerosol flow was diluted twice (total dilution ratio of 300) with ejector dilutors (Dekati, Finland) before it was sampled by a SP-AMS and a seven-wavelength (370–950 nm) aethalometer (AE33, Magee Scientific). A description of the aethalometer can be found in the SM along with a schematic illustration of the setup (Fig. S1). The residence time from the dilution system to sampling with the SP-AMS was about 3 s. High-molecular-weight PAHs are expected to equilibrate rapidly to the new conditions upon dilution (Hytonen et al., 2009). The SP-AMS measures only the particle phase of PAHs and not gas-phase species. Un-substituted PAHs with carbon numbers from 16 (MW = 202 Da) were included in the analysis. It is important to take into consideration that measurements of the particle phase of PAHs may be dependent on dilution ratio (at least for 4–5 ring PAHs).

2.2. Division into combustion phases and calculation of emission factors

The particulate emission of OA, PAH, *m/z* 60 and rBC_e showed strong variation over the combustion cycle. Based on the

combustion conditions, each cycle was divided into three phases following Eriksson et al. (2014): (1) the fuel addition phase (before flames appeared), (2) the intermediate (flaming) phase, and (3) the burnout phase. It should be emphasized that since wood log combustion is not completely homogenous, assigning phases to the combustion cycle is an idealization. More information concerning burn phases is found in SM, section 1.1.

In order to compare the different operation modes of the wood stove, the measured and dilution-adjusted particle concentrations (in mg/m³) were converted to emission factors for the full batches in [mg/kg_{batch}], where kg_{batch} is the dry weight of the wood logs in the full combustion batch. Emission factors were also evaluated for each combustion phase, [mg/kg_{phase}], where kg_{phase} refers to the dry weight of the fuel that is combusted in the combustion phase in question (fuel addition, intermediate, burn out phases). When calculating emission factors for NB, HB and VHB, 7, 6 and 3 cycles were used, respectively. The procedures to calculate the emission factors are described in more detail in SM, section 1.7.

2.3. Aerosol sampling and chemical quantification

The SP-AMS (Onasch et al., 2012) was used to measure the size-resolved chemical composition of submicron particles. In the SP-AMS the aerosols enter a vacuum system where they are vaporized, ionized with 70 eV electron ionization and detected with time-of-flight mass spectrometry. The SP-AMS has two vaporizers incorporated: (1) a tungsten surface heated to 600 °C, which vaporizes non-refractory particulate matter (PM), and (2) a continuous-wave 1064 nm intracavity Nd:YAG laser that enables vaporization of infrared light-absorbing aerosols, such as rBC (Onasch et al., 2012). In this study, the SP-AMS was primarily operated in dual vaporizer mode where both the laser and tungsten vaporizers are activated. Quantification of emissions is less established in the dual vaporizer mode (Ahern et al., 2016) compared to the tungsten vaporizer mode. To verify the quantification, a cycle of 10 min in dual vaporizer mode followed by a 2 min period with the laser switched off (tungsten vaporizer mode) was used throughout the campaign. Concentrations of particle phase PAHs, OA, rBC_e and *m/z* 60 were derived from the SP-AMS analysis.

The relative ionization efficiency (RIE) of rBC detected with the SP-AMS was first determined with the standard calibration procedures using Regal Black for rBC (dual vaporizer mode) and ammonium nitrate (tungsten vaporizer mode). The result for rBC was a RIE of 0.15. As the SP-AMS sensitivity to rBC depends on several factors (Ahern et al., 2016; Willis et al., 2014), we also compared the SP-AMS response to equivalent BC (eBC) measurements with an aethalometer, and to elemental carbon (EC) measurements with a thermal-optical method under steady state conditions. This was done when the intermediate phase biomass aerosol was sampled from a 17 m³ steel chamber. The results were an apparent collection efficiency (CE) of 0.50 when relating to eBC and a CE of 0.77 when relating to EC (Fig. S3). Several reports in the literature also found a reduced CE of rBC compared to Regal Black. Tiitta et al. (2016) found a reduced CE for rBC-dominated wood log emissions similar to those used in this study, and used an additional CE of 0.6. Ahern et al. (2016) found that thick SOA coatings on biomass combustion soot increased the sensitivity to rBC by a factor of 2.5 for the most relevant particle size for our study. Our data from the comparison with EC are quite uncertain (low number of samples and quite high scatter). Thus, on the basis of the literature and the comparison with eBC (which provides an apparent CE), we chose to use a CE of 0.5. This value has been applied for the full data set independent of burn phase and the term “rBC_e” will be used throughout the article where relevant to indicate that rBC_e is based on calibration with the aethalometer.

The method to quantify time-resolved PAH emissions from wood combustion was previously described by Eriksson et al. (2014). PAH quantification with the SP-AMS was also investigated by comparing it with PAH filter measurements using an in-house built, high-pressure liquid chromatograph coupled with a gas chromatographic system with a mass spectrometric detector (HPLC-GC-MS), as described in more detail in SM, section 1.3. The SP-AMS showed a factor of 1.5 higher in concentration compared to the reference method in measurements spanning more than two orders in concentration. The reported results were adjusted by this factor. Further information regarding the operation, data analysis, parameterization for quantification of PAHs and rBC_e (Figs. S2 and S3), and sensitivity of the SP-AMS along with the calculation of emission factors can be found in the SM.

3. Results and discussion

3.1. Time-resolved emissions

Representative cycles of emissions from the NB, HB and VHB experiments are presented in Fig. 1. The parameters considered are OA, PAH, rBC_e and $f60$ (fraction of OA signal for the ion $C_2H_4O_2^+$ at m/z 60), together with the content of the flue gases, O_2 and CO. The reason for the missing CO data during the intermediate phase for VHB is due to CO levels exceeding the maximum range for the instrument. Overall, the full cycles for all burning modes are dominated by rBC_e . For all burn modes, low temperature pyrolysis in the fuel addition phase results in strong, short-lived OA-dominated emissions, resulting in the highest peak concentrations of OA [mg/m^3] over the full cycle. $f60$ peaks just after the maximum OA concentration, showing that the relative fraction of levoglucosan and related compounds in OA increases as the fuel heats up before flames appear. However, as ignition is a poorly controlled process, the fuel addition phase emissions varied between cycles.

The intermediate phase for all burn modes is dominated by rBC_e emissions. OA is co-emitted with rBC_e but in lower concentrations compared to the fuel addition phase. The lowest concentrations of all species are found in the burn out phase where the organic matter emission rate from the wood logs approaches zero, and a progressively smaller fraction of the bed is covered with flames. At NB in the intermediate phase, the rBC_e emissions are relatively low but show considerable variability over time with no clear correlation with CO or O_2 . When comparing the different burn modes, one observes a positive correlation in the intermediate phase of rBC_e and PAHs in relation to the burn rates (VHB > HB > NB). VHB shows extremely high emissions of PAHs and elevated PM emissions in general. These increases, unlike for NB, are clearly associated with high CO emissions and low flue gas O_2 concentrations. In the intermediate phase, $f60$ is reduced with increasing burn rate.

3.2. Full cycle emission factors

The average full cycle emissions [mg/kg_{batch}] and the contributions from each of the three phases to the emissions of OA, rBC_e , PAH and m/z 60 are presented in Fig. 2 for NB, HB and VHB. The actual numbers are found in Table S3. The unit is mg/kg_{batch} , where kg_{batch} fuel refers to the dry weight of the whole fuel batch. The full cycle emission factors of rBC_e increased with increasing burn rate from 620 mg/kg_{batch} for NB to 1680 mg/kg_{batch} for VHB. rBC_e is the dominant species for full cycles at all burn rates, contributing approximately 66% for NB, 82% for HB, and 62% for VHB. Only for OA in the NB case did the contribution from fuel addition dominate the full cycle emissions. The average OA full cycle emission factor

increased from 330 (NB) to 900 mg/kg_{batch} (VHB), while the corresponding increase for m/z 60 was only a factor of 1.2. The rBC_e and OA emission factors at NB are similar to those reported in the literature (Tiitta et al., 2016) for a masonry heater (rBC 400–800 and OA 100–250 mg/kg_{batch}), and a conventional wood log stove operated with different fuels (EC 200–800 and OC 200–300 mg/kg_{batch}), and at an elevated burn rate (OC + EC = 2600 mg/kg_{batch}) (Orasche et al., 2012).

PAH emissions increased with increasing burn rate but in a much more dramatic way (compared to rBC_e and OA) from 3.4 mg/kg_{batch} (NB) to 225 mg/kg_{batch} (VHB). At HB and VHB the intermediate phase made by far the strongest contribution to the emission factor. Our relatively low particle-PAH emission factor for NB is in line with several studies using conventional time integrated filter techniques at nominal combustion conditions for wood stoves (Orasche et al., 2012) and masonry heaters (Tissari et al., 2007). The particle PAH emission factors at VHB are very high but similar to previous filter-based measurements for this (200 mg/kg_{batch} ; Pettersson et al., 2011) and another conventional wood stove operated at very high burn rates (120 mg/kg_{batch} ; Orasche et al., 2013). Strongly elevated PAH emissions (particle + gas phase) have also been reported by Hedberg et al. (2002): 280 mg/kg_{batch} for a conventional wood stove; and by Tissari et al. (2007): 164 mg/kg_{batch} for a sauna stove. The combustion conditions responsible for the very high PAH emissions in our study and potentially also those mentioned in the literature are discussed in detail in Section 3.5.

3.3. Emission factors for separate combustion phases and BC vs. brown carbon emissions

Fig. 3 presents emission factors (mg/kg_{phase}) of the individual combustion phases in each batch. The actual data used in the figure is given in Table S4. Here, the emitted PM is normalized to the dry weight of the fuel consumed in each combustion phase. This takes into account the large variations in burn rate/fuel consumption rate between the fuel addition and the intermediate phases. The fuel consumption (kg/s) is low during fuel addition so the emission factors (given as mg/kg_{phase}) become high. For example at NB, the emission factor (sum of OA + rBC_e) is about an order of magnitude higher during fuel addition (8500 mg/kg_{phase}) compared to the intermediate phase (770 mg/kg_{phase}). This clearly shows that prolonged low temperature pyrolysis may cause very high, primarily organic PM emissions, for example, in connection to a failed fuel addition when the batch is not correctly lighted (Corbin et al., 2015b), or when using humid fuels or poorly insulated stoves. Such high OA-dominated emissions and combustion conditions may also be relevant for open biomass burning and deforestation. Martinsson et al. (2015) recently reported for a sub-set of the data from the same campaign, that even if the PM_{10} mass emission factors were an order of magnitude higher for fuel addition (OA-dominated chemical composition and BrC-dominated light absorption) compared to flaming combustion (rBC -dominated chemical composition and BC-dominated light absorption), the light absorption emission factors were of a similar magnitude. Thus, BrC dominates fuel addition emissions while for the full cycle, absorption is dominated by BC.

At HB and VHB the differences in emission factors between the two phases are smaller due to reduced emissions during fuel addition and increased emissions during the intermediate phase. It is clearly shown that $f60$ in the intermediate phase is reduced with increasing burn rate. This has important implications for tracer methods based on levoglucosan as will be discussed in Section 3.6. The error bars (standard error of mean) in Fig. 3 indicate relatively

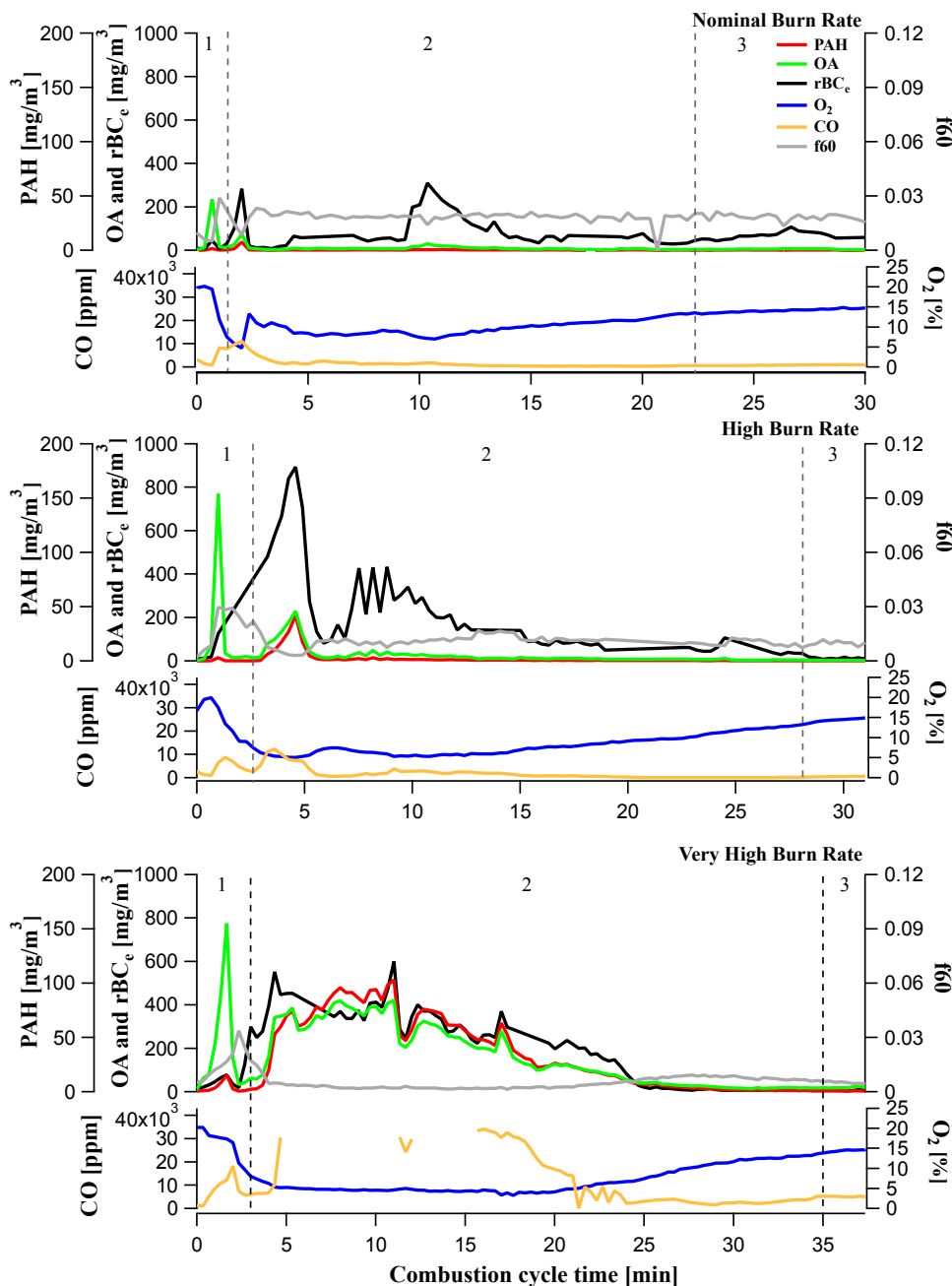


Fig. 1. Time series of particle phase OA, PAHs, rBC_e in mg/m³ and f60 (mass fraction of the ion C₂H₄O₂⁻ to OA; a marker of anhydrous sugars such as levoglucosan), CO [ppm] and O₂ [%] for nominal (top), high (middle), and very high burn rate (bottom). The two dotted lines in each graph divide the cycle into three phases: (1) fuel addition, (2) intermediate (flaming), and (3) burn out. The CO and O₂ averages for the batches in the figure were within 30% of the average for all batches included for NB, HB and VHB. Missing CO data during the intermediate phase for VHB is due to CO levels exceeding the maximum range for the instrument.

large variations between the different cycles for all burn modes. This reflects that a batch of fuel is never synchronized and that a total repeatability of cycles is close to impossible.

Few previous studies have quantified time-resolved PAH emissions in biomass combustion. Vicente et al. (2016) used conventional off-line filter sampling to sample PAH emissions from different parts of each combustion cycle in a wood stove. They concluded that the PAH emission factors were elevated 3–6 times during the first 10 min of each batch. This is largely consistent with our highly time-resolved data, commonly revealing PAH emission

peaks in the early intermediate phase and very low PAH emissions in the burn out phase.

3.4. Variation of chemical composition over particle size and mixing state

Chemically resolved mass size distributions varied considerably over individual burn cycles and between different burn rates (Fig. 4). The cycle-averaged rBC_e emissions were typically dominated by a size mode peaking between 100 and 200 nm (D_{va}:

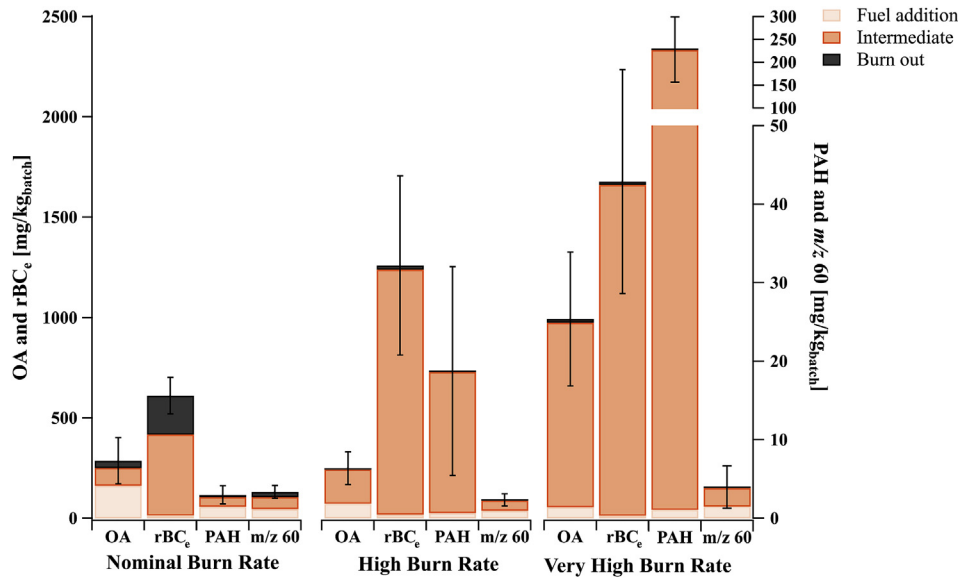


Fig. 2. Full cycle emission factors of OA, rBC_e, PAH and m/z 60 for nominal (NB), high (HB), and very high burn rate (VHB) in mg/kg_{batch}, where kg_{batch} fuel refers to the dry weight of the whole batch. The results are based on 7, 6 and 3 cycles, respectively. The contributions to the full cycle emissions are given for the three phases: fuel addition, intermediate, and burn out. Error bars represent the variation of the full cycles and are given as the standard error of the mean.

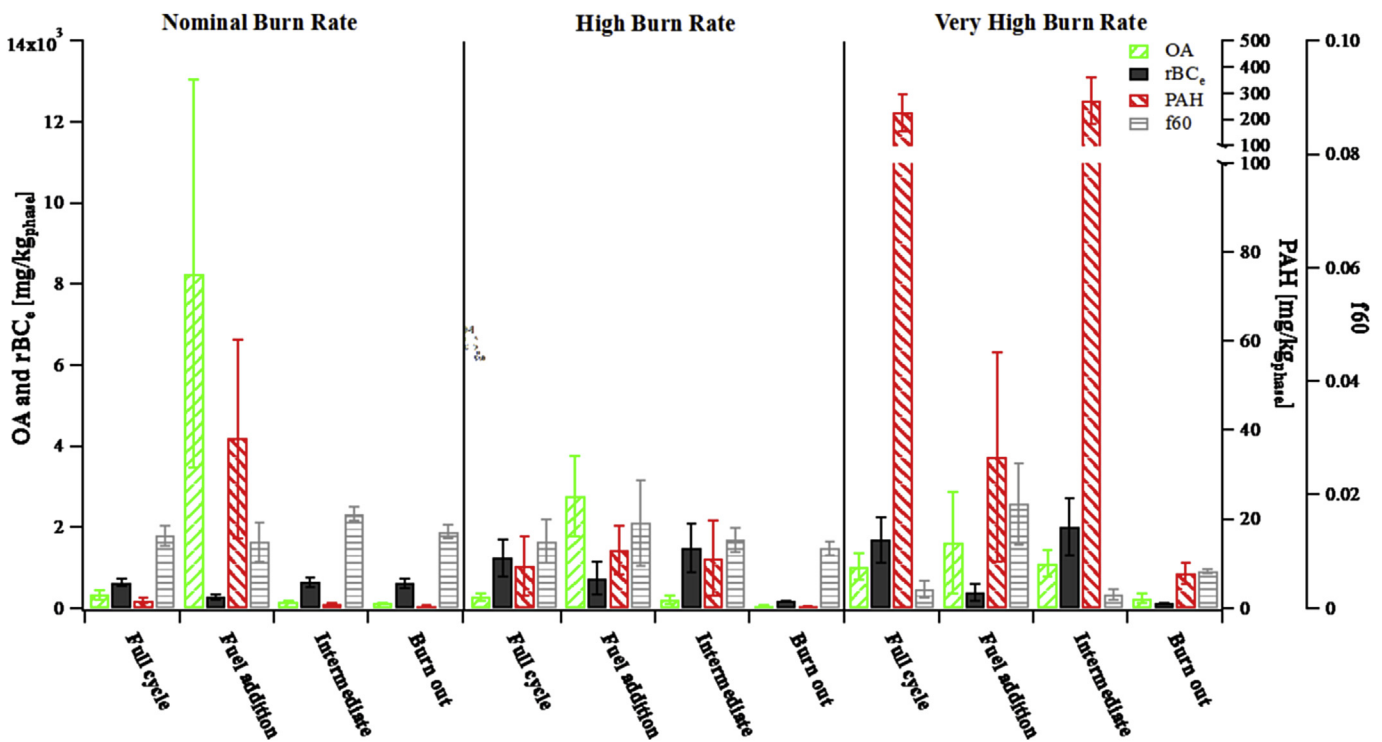


Fig. 3. Phase specific particulate emission factors of OA, rBC_e, PAH together with the mass fraction of OA at m/z 60, f60 (C₂H₄O₂), for nominal (NB), high (HB), and very high burn (VHB) rates in mg/kg_{phase} based on 7, 6 and 3 cycles, respectively. The calculations are given for the three phases: fuel addition, intermediate and burn out. The full cycle emission factor (in mg/kg_{batch}) is given for comparison. Error bars represent the variation between the cycles and are given as the standard error of the mean.

vacuum aerodynamic diameter). Notably, the peak of rBC is larger (in D_{va}) than the rBC observed in traffic emissions (Massoli et al., 2015). In addition, large OA-dominated particles showed a distinct peak at higher D_{va} (400–500 nm) in cycles that featured high OA fuel addition emission (an example is given for NB in Fig. 4b). Larger rBC_e-dominated particles were also present in the emissions, further discussed below.

As described in a separate publication (Martinsson et al., 2015), the bulk of the particles emitted in these experiments can be divided into two morphological categories based on transmission electron micrographs: agglomerated soot particles (consisting mostly of BC agglomerates) released in the intermediate (flaming) phase and spherical “tar ball” particles (organic) released during low temperature pyrolysis upon fuel addition. The sizing technique

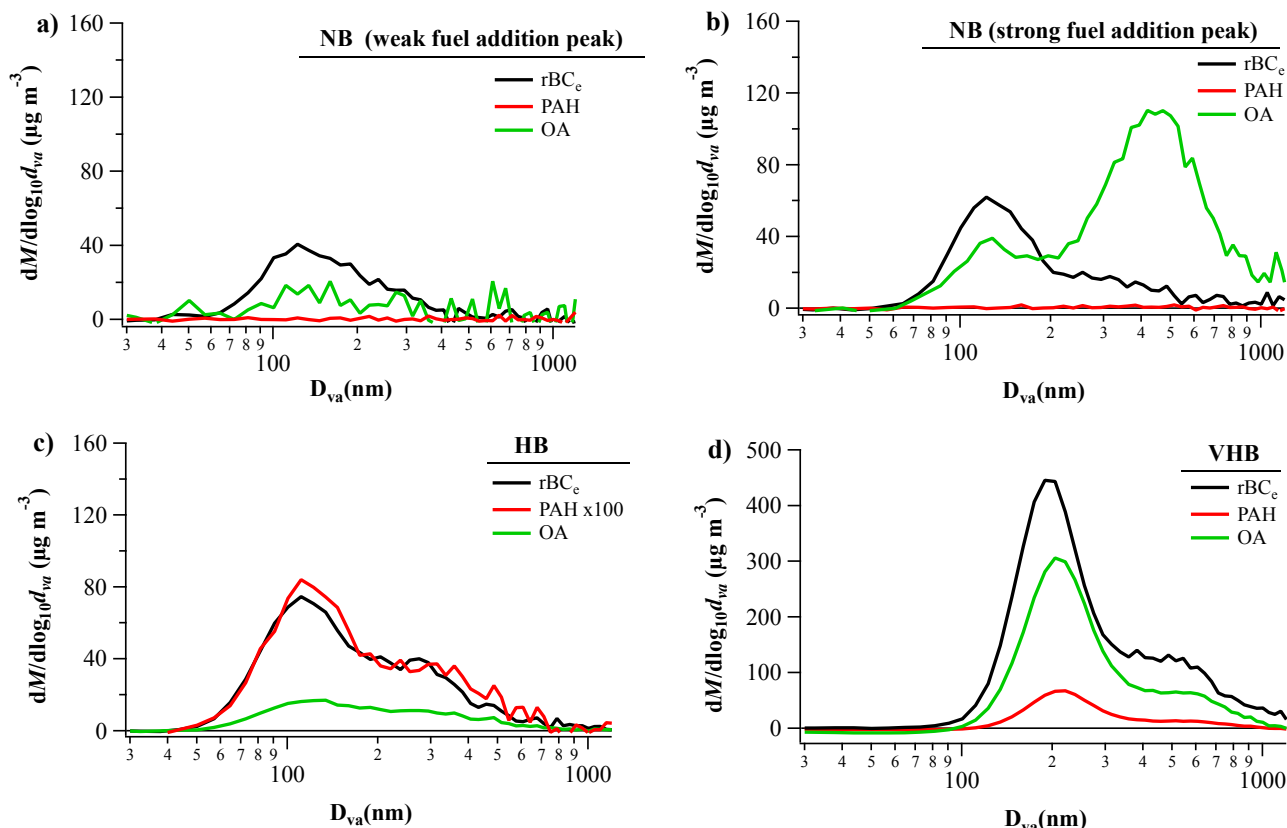


Fig. 4. Single cycle size-resolved emissions of rBC_e , OA and PAH. Examples for: (a) nominal (NB) for weak OA fuel addition peak, (b) nominal (NB) for strong OA fuel addition peak, (c) high (HB), and (d) very high (VHB) burn rate.

employed in the SP-AMS (aerodynamic sizing at low pressure; Jayne et al., 2000) is very sensitive to particle shape. Irregularly shaped particles, due to the strong drag forces they induce, appear smaller in size (DeCarlo et al., 2006). Thus, the SP-AMS can be used to separate these two particle types from on-line measurements and conclusions can be drawn about mixing state.

The smaller rBC_e mode (D_{va} around 100–200 nm) dominated 15 of the 16 cycles investigated. For these cycles, lognormal fits were made to rBC_e , excluding the larger sized contributions (Table S5). In order to investigate the variability in these emission modes, the fitted diameters were compared with the rBC_e mass fraction over the fitted size intervals (Fig. 5). By limiting the analysis to these size ranges (Table S5), only OA which was potentially internally mixed with the rBC_e was included in the calculation of the rBC_e fraction. It was found that a higher OA mass fraction (lower fraction rBC_e) was associated with higher D_{va} , as expected, assuming similar rBC_e cores (and internal mixing with OA) for the different cycles. However, there is significant scatter for high rBC_e fractions, which may be due to differing morphologies. In any case, the data clearly illustrate that the majority of the rBC_e particles emitted from this type of wood stove are thinly coated. This shows that atmospheric processing is needed for lensing-driven BC absorption amplification to occur. At HB and VHB, PAH and rBC_e distributions were similar, providing empirical evidence to support our previous hypothesis (Eriksson et al., 2014) of mainly internal mixtures of PAHs and rBC (for NB, the PAH size distributions were dominated by noise). The mixing state is also of importance when it comes to health effects, for example, the adsorption of PAHs to BC cores leads

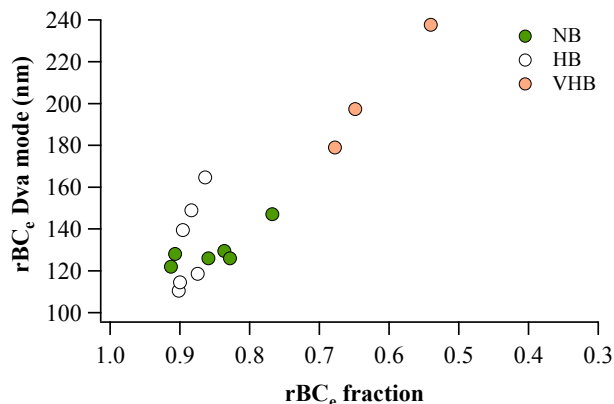


Fig. 5. Summary of fitted rBC_e mode diameter vs. rBC_e fraction from 15 cycles (details in text).

to increased genotoxic potency (Dilger et al., 2016).

Many cycles also had significant rBC_e contributions from even larger particles (>300 nm), resulting in highly asymmetric rBC_e distributions. We tentatively suggest this is due to soot particles with more aerodynamic shapes (e.g., more compact agglomerates). Coating produces more aerodynamic shapes; however, it is clear from the size distributions that the larger sized rBC_e (Fig. 4) is not simply more heavily coated rBC_e .

3.5. Interpretation of combustion conditions responsible for very high PAH emission episodes

Several authors have previously commented that high burn rates lead to increased emissions of PAHs (Eriksson et al., 2014; Orasche et al., 2013; Pettersson et al., 2011; Shen et al., 2013). The explanations of the relationship to combustion conditions have been quite brief, but several pointed out oxygen deficiencies in the stove at elevated burn rates. Here we present a deeper discussion that acknowledges the advances in gasification/pyrolysis and soot formation/oxidation research. At very high burn rates during the PAH emission peaks, the O₂ concentration in the flue gas is very low (2–4%, compared to ~10% at NB). The burn rate (fuel consumption rate) increases due to a larger fuel batch, dry fuel and smaller log sizes, but the air supply does not increase to the same extent. This is caused in the present setup by a combined effect of the natural draft design of the stove and the use of an ejector-based flue gas fan. This means that O₂ will be primarily consumed in the outer parts of the flame and near the air supply inlets. Thus, O₂ will be depleted in the central parts, resulting in an air deficient flame (air-to-fuel ratio $\ll 1$). We base our interpretation of the combustion conditions controlling the elevated PAH emissions on the following:

- 1) It is well known from both basic flame studies (Wang, 2011) and biomass gasification studies (Milne et al., 1998; Weiland et al., 2015) that the combustion temperature is reduced at low air-to-fuel ratios, that is, by endothermic gasification reactions.
- 2) It is well known from pyrolysis studies that the nature of the OA (tar) and gases shifts with increasing temperature, from primary pyrolysis products (such as levoglucosan), to phenols, to substituted single ring aromatics, and finally (at 900–1100 °C) large 4–5 ring PAHs that occur in the particle phase (Milne et al., 1998).
- 3) Soot/rBC formation proceeds by surface growth through the conversion/loss of large PAHs into soot by hydrogen abstraction (Wang, 2011). The conversion rate of PAHs to soot decreases rapidly when the local combustion temperature is reduced. Basic flame studies have shown strongly increased PAH emissions and PAH/rBC ratios from fuel rich premixed flames (Slowik et al., 2004). At temperatures of 900–1100 °C, essentially all tar components are converted to PAHs but the temperature is still too low for the efficient conversion of PAHs to soot at the relevant time scale of the flame.

The VHB combustion conditions in the wood stove fulfill the following: locally air-starved conditions, which lead to reduced flame temperatures, resulting in efficient PAH formation but a slow conversion of PAHs to rBC/soot on the relevant time scales. Alternatively, as the flame height increases due to the higher burn rate (i.e., increased flue/fuel gas flow) and with reduced combustion temperatures, the chance for flame quenching by the colder surfaces in the upper part of the stove and in the chimney will be high. Either way, as the flame is quenched or the O₂ concentration is reduced to locally very low values, the oxidation of the pollutants formed is effectively stopped and the available unburned pollutants are emitted. This facilitates the very high emissions of PAHs and the high PAH/rBC_e ratios at VHB. The situation with air-starved conditions in this kind of closed chimney stove is a well-known phenomenon that occurs in real-life operation.

During NB, PAH emissions in the intermediate phase are more than two orders of magnitude lower compared to VHB, while rBC_e emissions are only a factor of three lower. When the burn rate is lower, the oxygen availability is much higher, locally as well as globally, leading to higher combustion temperatures and reduced

flame heights. The conversion of PAHs to rBC_e becomes rapid compared to the residence time in the flame. Additionally, most of the rBC_e formed is efficiently oxidized and not emitted due to the high availability of oxidants in the oxidation regions in the flame. Still, flame quenching caused by convective air movements does occur. When the temperature is then rapidly decreased, un-burned pollutants escape further oxidation and are emitted in the chimney. However, this happens at a stage when the PAHs have been converted to rBC_e to a very high degree.

3.6. Interpretation of variations in f60 due to pyrolysis chemistry and implications for source apportionment with AMS

AMS is often used to apportion ambient OA into its main sources using approaches such as PMF and ME-2 (Crippa et al., 2013). With PMF, one typically finds a source factor denoted as biomass burning organic aerosol (BBOA) in which C₂H₄O₂⁺ (*m/z* 60) and C₃H₅O₂⁺ (*m/z* 73) are unique marker ions. Pure levoglucosan has a very high *m/z* 60 fraction of ~10% of the total OA signals (f60 = 0.10) (Alfarra et al., 2007). These two ions are weaker in BBOA from field experiments: ~2% (f60 = 0.02) and ~1% (f73 = 0.01), respectively (Crippa et al., 2013). We observed that the full batch emission factor based on *m/z* 60 was in principle independent of burn rate. However, f60 decreased from 0.013 to 0.003 for full cycle averages between NB and VHB. The f60 values for VHB are significantly lower than for ambient BBOA factors. Thus, the BBOA factor may underestimate the biomass contribution from VHB. In ambient measurements in polluted environments, PAH emissions have been attributed to sources by adding the total PAHs to the PMF analysis of AMS data (Elser et al., 2016). The SP-AMS also provides opportunities to include measurements of rBC and potentially also the refractory sulfates and chlorides (from potassium salts representing modern biomass combustion systems) to strengthen the AMS source profiles.

Corbin et al. (2015b) concluded that aerosol from the fuel addition phase was dominated by the pyrolysis products of cellulose and that intermediate phase OA emissions showed stronger contributions from pyrolysis products from lignin. They argued that the elevated organic emissions upon fuel addition were a result of pyrolysis below the ignition point, while the OA emissions in flaming combustion are a result of reaction products that have taken trajectories that avoided the flame throughout the combustion chamber. We found that the f60 was of similar magnitude in the fuel addition and the intermediate phase at both NB and HB (f60 = 0.010–0.016), in agreement with Corbin's hypothesis that OA emissions in the intermediate (flaming) phase have taken trajectories avoiding the flames. At VHB in the intermediate phase, f60 decreased due to the addition of high concentrations of PAHs and other aromatic components that originated from high temperature processes in the flame.

In the fuel addition phase we found that the f60 commonly increased as the fuel heats up and the pyrolysis rate increases with time. The maximum f60 appeared after the OA emission peak in agreement with previous studies (Elsasser et al., 2013). OA emission factors in the fuel addition phase decreased from 8200 mg/kg_{phase} at NB down to 1600 mg/kg_{phase} at VHB. At the same time there was a trend of increasing f60 from 0.012 (NB) to 0.018 (VHB). We also found that the average length of the fuel addition phase (until flaming combustion started) decreased from 190 s (NB) to 130 s (VHB) and that there was also a trend towards higher flue gas O₂ (the reduction of O₂ from ambient levels is a measure of the fuel conversion rate) during NB compared to VHB. This indicates that the pyrolysis rate increase from NB to VHB, is most likely due to the higher reactivity of the smaller and drier logs used at VHB. There was a strong variability of fuel addition OA emissions between

batches (from 200 up to 27,000 mg/kg_{phase}). Looking at individual batches, there was a relationship between increasing OA emission factors and the mean flue gas O₂ concentration in the fuel addition batch (Fig. S6). Finally, batches with very high OA emission factors (that strongly contribute to the total emissions) had reduced f60 (0.005; Fig. S6). Taken together, these results clearly suggest that the OA emission factor decreases and the f60 increases with increasing pyrolysis rate and temperature.

The main constituents of wood are volatilized in the following order (Shen et al., 2010): hemi-cellulose, cellulose, and lignin. Cellulose is by far the major source of levoglucosan and the levoglucosan yield passes a maximum at a temperature higher (~400 °C) than the volatilization temperature of cellulose (~350 °C). Major pyrolysis products for hemi-cellulose include mannosan, galactosan and xylosan. We therefore propose that the increase of f60 with increasing pyrolysis rate (temperature) is a result of increased levoglucosan yield with increasing temperature and possibly also due to a dominance of hemi-cellulose products with lower f60 than levoglucosan in OA at low pyrolysis rates (low temperatures).

3.7. Implications for filter-based source apportionment of biomass organic aerosol and particulate matter

The concentration of particulate wood combustion may be quantified by a receptor analysis of the ambient PM, frequently using a chemical mass balance (CMB) model (Miller et al., 1972; Watson et al., 1990) or a positive matrix factorization (PMF) model (Paatero, 1997). The choice of models depends on the amount and type of data, and on the knowledge one has of the contributing sources. Both models rely on conservation of mass, where the sum of sources with fixed profiles multiplied by their variable source strengths must equal the measured mass for any given species. As such, chemical reactions or repartitioning among markers as well as changes in sources and source compositions will violate these assumptions. Minor violations are handled with some penalty, which is reflected in the uncertainties of the apportioned sources. Ideally, the ratios of markers to PM should stay constant in ambient source profiles. Consequently, the same ratios should be

similar between burn cycles and burn rates in the laboratory experiments.

In order to test this, we correlated rBC_e, OA and *m/z* 60 to the PM₁ mass concentration, where OA and rBC_e account for the majority of the particulate mass. The sum of inorganic ions, including potassium, sulfate, chloride, nitrate and sodium, were analyzed with ion chromatography in our study and resulted in 80, 80 and 60 ± 20 mg/kg_{batch} for NB, HB and VHB, respectively (uncertainty given as std. Error of the mean). Additional components (including metals such as zinc) in PM₁ were estimated to 20 mg/kg_{batch} (Nordin et al., 2015). Full cycle OA and rBC_e both correlate with PM₁ (R² = 0.59 and 0.92, respectively, n = 16) regardless of burn rate (Fig. S5 and Table S6), however, not to the same extent.

Levoglucosan can account for as much as 14% of the wood combustion OA mass, and it has been demonstrated that levoglucosan and wood combustion OA are generally highly correlated (Elsasser et al., 2012). With regards to *m/z* 60, which represents levoglucosan (Simoneit et al., 1999), though other components may also significantly contribute (Heringa et al., 2011), there is a strong linear correlation (R² = 0.87, n = 7) with PM₁ at NB (Fig. 6a – the exact values can be found in Table S6). At HB and (more so) at VHB, the *m/z* 60 to PM₁ ratio is lower and also much more variable. This is due to increases in emissions of PM₁ and its main constituents (rBC_e and OA) with increasing burn rate, while the *m/z* 60 emissions are largely constant. Accordingly, levoglucosan may not accurately apportion wood combustion for all burning conditions, and this uncertainty adds to differences in levoglucosan formation arising from the burning of different types of wood (i.e., hardwood and softwood), and from modern combustion systems with reduced OA and levoglucosan emissions (Hedberg et al., 2006).

Particulate PAH emissions correlate moderately with PM₁ during NB and HB with a correlation coefficient squared of R² = 0.57 and a slope of 0.01. During VHB, the slope of PAHs vs. PM₁ increased approximately 13% (Fig. 6b). As discussed previously, the emissions of PAHs depend on several parameters (McDonald et al., 2000), where extensive flame quenching at high temperatures is expected to promote high emissions of complex particle phase PAHs as hypothesized in our study. The combustion conditions were widely different in VHB compared to NB, which is why the correlation

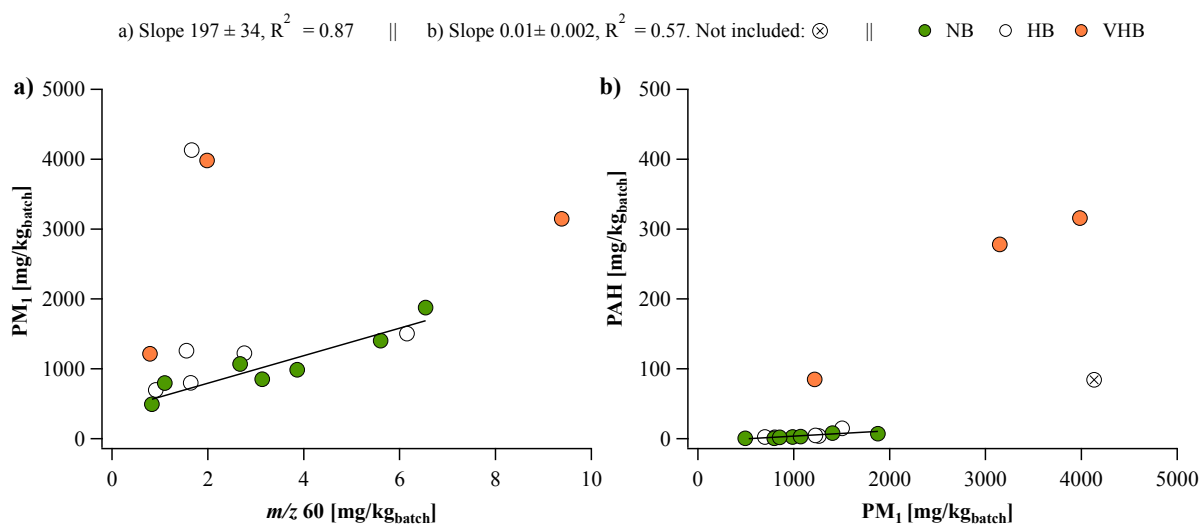


Fig. 6. a) Correlations for full combustion cycles between *m/z* 60 (“emission factor” for the concentration of C₂H₄O₂⁺ in the AMS mass spectra) and PM₁ in [mg/kg_{batch}] for nominal burn rate (NB), high (HB) and very high burn rate (VHB). HB and VHB data are presented in the graph but not included in the correlation. b) Correlations for full combustion cycles between PM₁ and particle phase PAHs [mg/kg_{batch}] for NB and HB. VHB data are presented in the graph but not included in the correlation. PM₁ is the sum of OA (incl. *m/z* 60), rBC_e, PAH, inorganic ions and metals.

between PAH and PM₁ was not expected during all burning modes. Fig. 6b further demonstrates how source apportionment using only PAHs can lead to erroneous conclusions. Rather, a more complex profile including levoglucosan, K (Harrison et al., 2012) (representing emissions from modern combustion systems, such as pellet boilers), BC and PAHs appears to be a more accurate approach for receptor modeling based on filter samples. Levoglucosan or K does not capture the increased emissions at high burn rates. However, adding PAHs and BC, or ratios such as levoglucosan/BC to the source profile in addition to MAS and K may capture these emissions in an improved way. Clearly, the use of source profiles representative of NB or HB on ambient wood combustion particles formed during conditions resembling VHB, could have no or very limited success. In realistic settings, atmospheric particles originating from biomass burning conditions that cover all burning modes will be present. This is unlikely to be matched in a single source profile. Where strong wood combustion sources representative of other burning conditions prevail, more wood combustion factors may be identified using PMF.

4. Conclusions and implications

Using time-resolved aerosol mass spectrometry, we reported emission factors of rBC_e, OA and particle phase PAHs from a conventional wood log stove from nominal burn rates up to very high burn rates. Full batch emissions increased by factors of ~3, 3 and 70 for rBC_e, OA and PAHs, respectively, and were largely in agreement with the literature data. The time-resolved technique allowed us to report separate emission factors for three combustion phases in each batch. PM₁ emission factors in the fuel addition phase (low temperature pyrolysis) were OA-dominated and up to an order of magnitude higher compared to the rBC_e-dominated emissions from the intermediate (flaming) phase. Thus, the highest mass emission factors from residential wood combustion are caused by low temperature pyrolysis, which may be part of the explanation as to why ambient aerosols dominated by wood combustion are OA and not rBC_e dominated. Emissions of tracers based on anhydrous sugars such as levoglucosan (based on *m/z* 60 in AMS spectra) were, unlike OA, rBC_e and PAHs, in principle unchanged with increasing burn rates, which has implications for source apportionment studies.

The mechanisms causing the strongly elevated PAH emissions at VHB were discussed based on knowledge from gasification/pyrolysis and soot formation/oxidation studies and interpreted to result from reduced flame temperatures due to locally air-starved conditions, which slow down the transformation of PAHs to soot/rBC. The situation with air-starved conditions in this kind of closed chimney stove is a well-known phenomenon that occurs in real-life operation. These combustion conditions may also be relevant to explain the very high PAH emissions found in field measurements of emissions from Chinese biomass cook stoves (Guofeng et al., 2013). We also reported trends between pyrolysis rates/temperatures, OA emission factors and *m/z* 60 at low temperature pyrolysis.

We showed that the SP-AMS in the size-resolved mode can separate emissions occurring at flaming combustion from those occurring during low temperature pyrolysis during fuel addition. The results showed that in the wood stove investigated here, flaming combustion led to thinly coated BC aggregates, while low temperature pyrolysis led to OA-dominated particles. This implies that the BC emitted during flaming combustion has no or low absorption enhancement in the atmosphere due to lensing.

Martinsson et al. (2015) showed for a subset of the data in this study a lower OA emission factor along with higher SOA formation potential and higher OA mass absorption coefficients in the UV range in experiments with high f60 compared to experiments with low f60. We anticipate that future studies include controlled

pyrolysis experiments that can establish relationships between pyrolysis temperature and aerosol properties on the one hand, and climate and health relevant properties (MAC of OA, SOA formation potentials, emissions of PAHs and other genotoxic compounds) on the other. Fundamental links between combustion conditions and emission characteristics can also be transferred between technologies. For example, fundamental studies of pyrolysis may provide generalizable information of relevance for emissions from wood stoves, cook stoves and smoldering combustion in forest fires or during deforestation.

Funding

This study was supported by the Arctic Centre of Research at Aarhus University, by the Cryosphere-Atmosphere Interaction in a Changing Arctic Climate (CRAICC) initiative, and by the WOOD Combustion Project – Detailed Monitoring Related to Acute Effects in Denmark (WOODMAD) as funded by the Danish Environmental Protection Agency. The Swedish Research Council VR project nr. 2013-5021 and the Research Council Formas project nr. 2013-1023 are greatly acknowledge for financial support of the Lund University and Umeå University contributions.

Appendix A. Supplementary data

Supplementary data related to this article can be found at <http://dx.doi.org/10.1016/j.atmosenv.2017.06.033>.

References

- Ahern, A.T., Subramanian, R., Saliba, G., Lipsky, E.M., Donahue, N.M., Sullivan, R.C., 2016. Effect of secondary organic aerosol coating thickness on the real-time detection and characterization of biomass-burning soot by two particle mass spectrometers. *Atmos. Meas. Tech.* 9, 6117–6137.
- Alfarra, M.R., Prevot, A.S.H., Szidat, S., Sandradewi, J., Weimer, S., Lanz, V.A., Schreiber, D., Mohr, M., Baltensperger, U., 2007. Identification of the mass spectral signature of organic aerosols from wood burning emissions. *Environ. Sci. Technol.* 41, 5770–5777.
- Boman, C., Nordin, A., Thaning, L., 2003. Effects of increased biomass pellet combustion on ambient air quality in residential areas - a parametric dispersion modeling study. *Biomass Bioenergy* 24, 465–474.
- Bond, T.C., Doherty, S.J., Fahey, D.W., Forster, P.M., Bernsten, T., DeAngelo, B.J., Flanner, M.G., Ghan, S., Karcher, B., Koch, D., Kinne, S., Kondo, Y., Quinn, P.K., Sarofim, M.C., Schultz, M.G., Schulz, M., Venkataraman, C., Zhang, H., Zhang, S., Bellouin, N., Guttikunda, S.K., Hopke, P.K., Jacobson, M.Z., Kaiser, J.W., Klimont, Z., Lohmann, U., Schwarz, J.P., Shindell, D., Storelvmo, T., Warren, S.G., Zender, C.S., 2013. Bounding the role of black carbon in the climate system: a scientific assessment. *J. Geophys. Res. Atmos.* 118, 5380–5552.
- Corbin, J.C., Keller, A., Lohmann, U., Bartscher, H., Sierau, B., Mensah, A.A., 2015a. Organic emissions from a wood stove and a pellet stove before and after simulated atmospheric aging. *Aerosol Sci. Technol.* 49, 1037–1050.
- Corbin, J.C., Lohmann, U., Sierau, B., Keller, A., Bartscher, H., Mensah, A.A., 2015b. Black carbon surface oxidation and organic composition of beech-wood soot aerosols. *Atmos. Chem. Phys.* 15, 11885–11907.
- Crippa, M., DeCarlo, P.F., Slowik, J.G., Mohr, C., Heringa, M.F., Chirico, R., Poulain, L., Freutel, F., Sciare, J., Cozic, J., Di Marco, C.F., Elsasser, M., Nicolas, J.B., Marchand, N., Abidi, E., Wiedensohler, A., Drewnick, F., Schneider, J., Borrmann, S., Nemitz, E., Zimmermann, R., Jaffrezo, J.L., Prevot, A.S.H., Baltensperger, U., 2013. Wintertime aerosol chemical composition and source apportionment of the organic fraction in the metropolitan area of Paris. *Atmos. Chem. Phys.* 13, 961–981.
- DeCarlo, P.F., Kimmel, J.R., Trimborn, A., Northway, M.J., Jayne, J.T., Aiken, A.C., Gonin, M., Fuhrer, K., Horvath, T., Docherty, K.S., Worsnop, D.R., Jimenez, J.L., 2006. Field-deployable, high-resolution, time-of-flight aerosol mass spectrometer. *Anal. Chem.* 78, 8281–8289.
- Dilger, M., Orasche, J., Zimmermann, R., Paur, H.R., Diabate, S., Weiss, C., 2016. Toxicity of wood smoke particles in human A549 lung epithelial cells: the role of PAHs, soot and zinc. *Arch. Toxicol.* 90 (12), 3029–3044.
- Elsasser, M., Busch, C., Orasche, J., Schön, C., Hartmann, H., Schnelle-Kreis, J., Zimmermann, R., 2013. Dynamic changes of the aerosol composition and concentration during different burning phases of wood combustion. *Energy Fuels* 27, 4959–4968.
- Elsasser, M., Crippa, M., Orasche, J., DeCarlo, P.F., Oster, M., Pitz, M., Cyrus, J., Gustafson, T.L., Pettersson, J.B.C., Schnelle-Kreis, J., Prevot, A.S.H., Zimmermann, R., 2012. Organic molecular markers and signature from wood

- combustion particles in winter ambient aerosols: aerosol mass spectrometer (AMS) and high time-resolved GC-MS measurements in Augsburg. *Ger. Atmos. Chem. Phys.* 12, 6113–6128.
- Elsner, M., Huang, R.J., Wolf, R., Slowik, J.G., Wang, Q.Y., Canonaco, F., Li, G.H., Bozzetti, C., Daellenbach, K.R., Huang, Y., Zhang, R.J., Li, Z.Q., Cao, J.J., Baltensperger, U., El-Haddad, I., Prevot, A.S.H., 2016. New insights into PM_{2.5} chemical composition and sources in two major cities in China during extreme haze events using aerosol mass spectrometry. *Atmos. Chem. Phys.* 16, 3207–3225.
- Engling, G., Carrico, C.M., Kreidenweis, S.M., Collett, J.L., Day, D.E., Malm, W.C., Lincoln, E., Hao, W.M., Iinuma, Y., Herrmann, H., 2006. Determination of levoglucosan in biomass combustion aerosol by high-performance anion-exchange chromatography with pulsed amperometric detection. *Atmos. Environ.* 40, 299–311.
- Eriksson, A.C., Nordin, E.Z., Nystrom, R., Pettersson, E., Swietlicki, E., Bergvall, C., Westerholm, R., Boman, C., Pagels, J.H., 2014. Particulate PAH emissions from residential biomass combustion: time-resolved analysis with aerosol mass spectrometry. *Environ. Sci. Technol.* 48, 7143–7150.
- Fine, P.M., Cass, G.R., Simoneit, B.R.T., 2002. Chemical characterization of fine particle emissions from the fireplace combustion of woods grown in the southern United States. *Environ. Sci. Technol.* 36, 1442–1451.
- Fine, P.M., Cass, G.R., Simoneit, B.R.T., 2004. Chemical characterization of fine particle emissions from the wood stove combustion of prevalent United States tree species. *Environ. Eng. Sci.* 21, 705–721.
- Gelencser, A., May, B., Simpson, D., Sanchez-Ochoa, A., Kasper-Giebl, A., Puxbaum, H., Caseiro, A., Pio, C., Legrand, M., 2007. Source apportionment of PM_{2.5} organic aerosol over Europe: primary/secondary, natural/anthropogenic, and fossil/biogenic origin. *J. Geophys. Res. Atmos.* 112.
- Genberg, J., Hyder, M., Stenstrom, K., Bergstrom, R., Simpson, D., Fors, E.O., Jonsson, J.A., Swietlicki, E., 2011. Source apportionment of carbonaceous aerosol in southern Sweden. *Atmos. Chem. Phys.* 11, 11387–11400.
- Guofeng, R., Feng, T., Lin, Y., 2013. The research of thermal design for vehicle controller based on simulation. *Appl. Therm. Eng.* 58, 420–429.
- Harrison, R.M., Beddows, D.C.S., Hu, L., Yin, J., 2012. Comparison of methods for evaluation of wood smoke and estimation of UK ambient concentrations. *Atmos. Chem. Phys.* 12, 8271–8283.
- Hedberg, E., Johansson, C., Johansson, L., Swietlicki, E., Brorström-Lundén, E., 2006. Is levoglucosan a suitable quantitative tracer for wood burning? Comparison with receptor modeling on trace elements in Lycksele, Sweden. *J. Air Waste Manage. Assoc.* 56, 1669–1678.
- Hedberg, E., Kristensson, A., Ohlsson, M., Johansson, C., Johansson, P.A., Swietlicki, E., Vesely, V., Wideqvist, U., Westerholm, R., 2002. Chemical and physical characterization of emissions from birch wood combustion in a wood stove. *Atmos. Environ.* 36, 4823–4837.
- Hennigan, C.J., Miracolo, M.A., Engelhart, G.J., May, A.A., Presto, A.A., Lee, T., Sullivan, A.P., McMeeking, G.R., Coe, H., Wold, C.E., Hao, W.M., Gilman, J.B., Kuster, W.C., de Gouw, J., Schichtel, B.A., Collett, J.L., Kreidenweis, S.M., Robinson, A.L., 2011. Chemical and physical transformations of organic aerosol from the photo-oxidation of open biomass burning emissions in an environmental chamber. *Atmos. Chem. Phys.* 11, 7669–7686.
- Hennigan, C.J., Sullivan, A.P., Collett, J.L., Robinson, A.L., 2010. Levoglucosan stability in biomass burning particles exposed to hydroxyl radicals. *Geophys. Res. Lett.* 37, L09806.
- Heringa, M.F., DeCarlo, P.F., Chirico, R., Lauber, A., Doberer, A., Good, J., Nussbaumer, T., Keller, A., Burtscher, H., Richard, A., Miljevic, B., Prevot, A.S.H., Baltensperger, U., 2012. Time-resolved characterization of primary emissions from residential wood combustion appliances. *Environ. Sci. Technol.* 46, 11418–11425.
- Heringa, M.F., DeCarlo, P.F., Chirico, R., Tritscher, T., Dommen, J., Weingartner, E., Richter, R., Wehrle, G., Prevot, A.S.H., Baltensperger, U., 2011. Investigations of primary and secondary particulate matter of different wood combustion appliances with a high-resolution time-of-flight aerosol mass spectrometer. *Atmos. Chem. Phys.* 11, 5945–5957.
- Hytonen, K., Yli-Pirila, P., Tissari, J., Grohn, A., Riipinen, I., Lehtinen, K.E.J., Jokiniemi, J., 2009. Gas-particle distribution of PAHs in wood combustion emission determined with annular denuders, filter, and polyurethane foam adsorbent. *Aerosol Sci. Technol.* 43, 442–454.
- Janssen, N.A.H., Hoek, G., Simic-Lawson, M., Fischer, P., van Bree, L., ten Brink, H., Keuken, M., Atkinson, R.W., Anderson, H.R., Brunekreef, B., Cassee, F.R., 2011. Black carbon as an additional indicator of the adverse health effects of airborne particles compared with PM₁₀ and PM_{2.5}. *Environ. Health Perspect.* 119, 1691–1699.
- Jayne, J.T., Leard, D.C., Zhang, X., Davidovits, P., Smith, K.A., Kolb, C.E., Worsnop, D.R., 2000. Development of an aerosol mass spectrometer for size and composition analysis of submicron particles. *Aerosol Sci. Technol.* 33, 49–70.
- Leskinen, J., Ihalainen, M., Torvela, T., Kortelainen, M., Lamberg, H., Tiitta, P., Jakobi, G., Grigonyte, J., Joutsensaari, J., Sippula, O., Tissari, J., Virtanen, A., Zimmermann, R., Jokiniemi, J., 2014. Effective density and morphology of particles emitted from small-scale combustion of various wood fuels. *Environ. Sci. Technol.* 48, 13298–13306.
- Liu, S., Aiken, A.C., Gorkowski, K., Dubey, M.K., Cappa, C.D., Williams, L.R., Herndon, S.C., Massoli, P., Fortner, E.C., Chhabra, P.S., Brooks, W.A., Onasch, T.B., Jayne, J.T., Worsnop, D.R., China, S., Sharma, N., Mazzoleni, C., Xu, L., Ng, N.L., Liu, D., Allan, J.D., Lee, J.D., Fleming, Z.L., Mohr, C., Zotter, P., Szidat, A., Prevot, A.S.H., 2015. Enhanced light absorption by mixed source black and brown carbon particles in UK winter. *Nat. Commun.* 6 (No. 8435).
- Martinsson, J., Eriksson, A.C., Nielsen, I.E., Malmberg, V.B., Ahlberg, E., Andersen, C., Lindgren, R., Nystrom, R., Nordin, E.Z., Brune, W.H., Svenningsson, B., Swietlicki, E., Boman, C., Pagels, J.H., 2015. Impacts of combustion conditions and photochemical processing on the light absorption of biomass combustion aerosol. *Environ. Sci. Technol.* 49, 14663–14671.
- Massoli, P., Onasch, T.B., Cappa, C.D., Nuamaan, I., Hakala, J., Hayden, K., Li, S.M., Sueper, D.T., Bates, T.S., Quinn, P.K., Jayne, J.T., Worsnop, D.R., 2015. Characterization of black carbon-containing particles from soot particle aerosol mass spectrometer measurements on the R/V Atlantis during CalNex 2010. *J. Geophys. Res. Atmos.* 120, 2575–2593.
- McDonald, J.D., Zielinska, B., Fujita, E.M., Sagebiel, J.C., Chow, J.C., Watson, J.G., 2000. Fine particle and gaseous emission rates from residential wood combustion. *Environ. Sci. Technol.* 34, 2080–2091.
- Miller, M.S., Friedlander, S.K., Hidy, G.M., 1972. Chemical element balance for Pasadena aerosol. *J. Colloid Interface Sci.* 39, 165–176.
- Milne, T.A., Abatzoglou, N., Evans, R.J., 1998. Biomass Gasifier "Tars": Their Nature, Formation, and Conversion. Technical Report for National Renewable Energy Laboratory, Golden, Colorado.
- Naeher, L.P., Brauer, M., Lipsett, M., Zelikoff, J.T., Simpson, C.D., Koenig, J.Q., Smith, K.R., 2007. Woodsmoke health effects: a review. *Inhal. Toxicol.* 19, 67–106.
- Nordin, E.Z., Uski, O., Nystrom, R., Jalava, P., Eriksson, A.C., Genberg, J., Roldin, P., Bergvall, C., Westerholm, R., Jokiniemi, J., Pagels, J.H., Boman, C., Hirvonen, M.R., 2015. Influence of ozone initiated processing on the toxicity of aerosol particles from small scale wood combustion. *Atmos. Environ.* 102, 282–289.
- Onasch, T.B., Trimborn, A., Fortner, E.C., Jayne, J.T., Kok, G.L., Williams, L.R., Davidovits, P., Worsnop, D.R., 2012. Soot particle aerosol mass spectrometer: development, validation, and initial application. *Aerosol Sci. Technol.* 46, 804–817.
- Orasche, J., Schnelle-Kreis, J., Schon, C., Hartmann, H., Ruppert, H., Arteaga-Salas, J.M., Zimmermann, R., 2013. Comparison of emissions from wood combustion. Part 2: impact of combustion conditions on emission factors and characteristics of particle-bound organic species and polycyclic aromatic hydrocarbon (PAH)-Related toxicological potential. *Energy Fuels* 27, 1482–1491.
- Orasche, J., Seidel, T., Hartmann, H., Schnelle-Kreis, J., Chow, J.C., Ruppert, H., Zimmermann, R., 2012. Comparison of emissions from wood combustion. Part 1: emission factors and characteristics from different small-scale residential heating appliances considering particulate matter and polycyclic aromatic hydrocarbon (PAH)-Related toxicological potential of particle-bound organic species. *Energy Fuels* 26, 6695–6704.
- Paatero, P., 1997. Least squares formulation of robust non-negative factor analysis. *Chemom. Intell. Lab. Syst.* 37, 23–35.
- Pagels, J., Dutcher, D.D., Stolzenburg, M.R., McMurry, P.H., Galli, M.E., Gross, D.S., 2013. Fine-particle emissions from solid biofuel combustion studied with single-particle mass spectrometry: identification of markers for organics, soot, and ash components. *J. Geophys. Res. Atmos.* 118, 859–870.
- Pettersson, E., Boman, C., Westerholm, R., Bostrom, D., Nordin, A., 2011. Stove performance and emission characteristics in residential wood log and pellet combustion. Part 2: wood stove. *Energy Fuels* 25, 315–323.
- Sarigiannis, D.A., Karakitsios, S.P., Zikopoulos, D., Nikolaki, S., Kermenidou, M., 2015. Lung cancer risk from PAHs emitted from biomass combustion. *Environ. Res.* 137, 147–156.
- Shen, D.K., Gu, S., Bridgwater, A.V., 2010. The thermal performance of the polysaccharides extracted from hardwood: cellulose and hemicellulose. *Carbohydr. Polym.* 82, 39–45.
- Shen, G.F., Xue, M., Wei, S.Y., Chen, Y.C., Zhao, Q.Y., Li, B., Wu, H.S., Tao, S., 2013. Influence of fuel moisture, charge size, feeding rate and air ventilation conditions on the emissions of PM, OC, EC, parent PAHs, and their derivatives from residential wood combustion. *J. Environ. Sci-China* 25, 1808–1816.
- Sigsgaard, T., Forsberg, B., Annesi-Maesano, I., Blomberg, A., Bolling, A., Boman, C., Bonlokke, J., Brauer, M., Bruce, N., Heroux, M.E., Hirvonen, M.R., Kelly, F., Kunzli, N., Lundback, B., Moshhammer, H., Noonan, C., Pagels, J., Sallsten, G., Sculier, J.P., Brunekreef, B., 2015. Health impacts of anthropogenic biomass burning in the developed world. *Eur. Respir. J.* 46, 1577–1588.
- Simoneit, B.R.T., 2002. Biomass burning - a review of organic tracers for smoke from incomplete combustion. *Appl. Geochem.* 17, 129–162.
- Simoneit, B.R.T., Schauer, J.J., Nolte, C.G., Oros, D.R., Elias, V.O., Fraser, M.P., Rogge, W.F., Cass, G.R., 1999. Levoglucosan, a tracer for cellulose in biomass burning and atmospheric particles. *Atmos. Environ.* 33, 173–182.
- Slowik, J.G., Stankin, K., Davidovits, P., Williams, L.R., Jayne, J.T., Kolb, C.E., Worsnop, D.R., Rudich, Y., DeCarlo, P.F., Jimenez, J.L., 2004. Particle morphology and density characterization by combined mobility and aerodynamic diameter measurements. Part 2: application to combustion-generated soot aerosols as a function of fuel equivalence ratio. *Aerosol Sci. Technol.* 38, 1206–1222.
- Tiitta, P., Leskinen, A., Hao, L.Q., Yli-Pirila, P., Kortelainen, M., Grigonyte, J., Tissari, J., Lamberg, H., Hartikainen, A., Kuusipalo, K., Kortelainen, A.M., Virtanen, A., Lehtinen, K.E.J., Komppula, M., Pieber, S., Prevot, A.S.H., Onasch, T.B., Worsnop, D.R., Czech, H., Zimmermann, R., Jokiniemi, J., Sippula, O., 2016. Transformation of logwood combustion emissions in a smog chamber: formation of secondary organic aerosol and changes in the primary organic aerosol upon daytime and nighttime aging. *Atmos. Chem. Phys.* 16, 13251–13269.
- Tissari, J., Hytonen, K., Lyyranen, J., Jokiniemi, J., 2007. A novel field measurement method for determining fine particle and gas emissions from residential wood combustion. *Atmos. Environ.* 41, 8330–8344.

- Vicente, E.D., Vicente, A.M., Bandowe, B.A.M., Alves, C.A., 2016. Particulate phase emission of parent polycyclic aromatic hydrocarbons (PAHs) and their derivatives (alkyl-PAHs, oxygenated-PAHs, azaarenes and nitrated PAHs) from manually and automatically fired combustion appliances. *Air Qual. Atmos. Hlth* 9, 653–668.
- Wang, H., 2011. Formation of nascent soot and other condensed-phase materials in flames. *P Combust. Inst.* 33, 41–67.
- Watson, J.G., Robinson, N.F., Chow, J.C., 1990. The USEPA/DRI chemical mass balance receptor model, CMB 7.0. *Environ. Softw.* 5, 38–49.
- Weiland, F., Wiinikka, H., Hedman, H., Wennebro, J., Pettersson, E., Gebart, R., 2015. Influence of process parameters on the performance of an oxygen blown entrained flow biomass gasifier. *Fuel* 153, 510–519.
- Weimer, S., Alfarra, M.R., Schreiber, D., Mohr, M., Prevot, A.S.H., Baltensperger, U., 2008. Organic aerosol mass spectral signatures from wood-burning emissions: influence of burning conditions and wood type. *J. Geophys. Res. Atmos.* 113.
- Willis, M.D., Lee, A.K.Y., Onasch, T.B., Fortner, E.C., Williams, L.R., Lambe, A.T., Worsnop, D.R., Abbatt, J.P.D., 2014. Collection efficiency of the soot-particle aerosol mass spectrometer (SP-AMS) for internally mixed particulate black carbon. *Atmos. Meas. Tech.* 7, 4507–4516.
- Wöhler, M., Andersen, J.S., Becker, G., Persson, H., Reichert, G., Schön, C., Schmidl, C., Jaeger, D., Pelz, S.K., 2016. Investigation of real life operation of biomass room heating appliances – results of a European survey. *Appl. Energy* 169, 240–249.
- Yttri, K.E., Simpson, D., Nojgaard, J.K., Kristensen, K., Genberg, J., Stenstrom, K., Swietlicki, E., Hillamo, R., Aurela, M., Bauer, H., Offenberg, J.H., Jaoui, M., Dye, C., Eckhardt, S., Burkhardt, J.F., Stohl, A., Glasius, M., 2011. Source apportionment of the summer time carbonaceous aerosol at Nordic rural background sites. *Atmos. Chem. Phys.* 11, 13339–13357.
- Zdrahal, Z., Oliveira, J., Vermeylen, R., Claeys, M., Maenhaut, W., 2002. Improved method for quantifying levoglucosan and related monosaccharide anhydrides in atmospheric aerosols and application to samples from urban and tropical locations. *Environ. Sci. Technol.* 36, 747–753.